

## Valence band XPS and UPS studies of non-stoichiometric superconducting $\text{NbB}_{2+x}$

This article has been downloaded from IOPscience. Please scroll down to see the full text article.

2012 Supercond. Sci. Technol. 25 015002

(<http://iopscience.iop.org/0953-2048/25/1/015002>)

View [the table of contents for this issue](#), or go to the [journal homepage](#) for more

Download details:

IP Address: 132.248.12.211

The article was downloaded on 18/09/2013 at 19:27

Please note that [terms and conditions apply](#).

# Valence band XPS and UPS studies of non-stoichiometric superconducting $\text{NbB}_{2+x}$

R Escamilla, L Huerta, F Morales and T Akachi

Instituto de Investigaciones en Materiales, Universidad Nacional Autónoma de México, Apartado Postal 70-360, México DF, 04510, Mexico

E-mail: [rauleg@unam.mx](mailto:rauleg@unam.mx)

Received 5 August 2011, in final form 11 October 2011

Published 5 December 2011

Online at [stacks.iop.org/SUST/25/015002](http://stacks.iop.org/SUST/25/015002)

## Abstract

The electronic structure of non-stoichiometric superconducting  $\text{NbB}_{2+x}$  has been investigated by x-ray photoelectron spectroscopy (XPS) and ultraviolet photoelectron spectroscopy (UPS). The analysis of the valence band using XPS and UPS reveals that the boron doping induces a systematic decrease in the density of states at Fermi level  $N(E_F)$  similar to that observed in the  $\text{Nb}_{1-x}\text{B}_2$  system. In particular,  $N(E_F)$  is lower for the superconducting samples than for the non-superconducting ones. In the superconducting samples, we confirm that the  $T_c$  is inversely proportional to  $N(E_F)$ . Therefore, the presence of superconductivity in these samples cannot be explained only as a function of the  $N(E_F)$ . Thus, the presence of superconductivity in our samples might be explained by increases in the number of holes in-plane conduction, due to an increase in the number of niobium vacancies as boron content is increased.

(Some figures may appear in colour only in the online journal)

## 1. Introduction

The discovery of superconductivity in  $\text{MgB}_2$  at about 40 K by Nagamatsu *et al* [1] generated a great deal of excitement, and many studies related to both fundamental and practical aspects have been reported. Superconductivity in the metal borides with an  $\text{AlB}_2$ -type structure has been studied for several decades [2, 3]. In 1970, Cooper *et al* reported the presence of superconductivity in the Nb–B and Mo–B compounds, and they noted also that the stoichiometric compounds  $\text{NbB}_2$  and  $\text{MoB}_2$  were non-superconductors [4]. Here, much interest has been paid to the group V transition metal diborides, especially to the hexagonal  $\text{NbB}_2$ .

In previous studies on  $\text{NbB}_2$  it was shown that in Nb-deficient samples the transition temperature ( $T_c$ ) increases up to around 9.2 K [5], while in B-excess samples the highest  $T_c$  is 9.8 K for the composition (B/Nb) = 2.34 [6]. X-ray photoelectron spectroscopy studies on B-excess samples have shown that: (a) the binding energies of the Nb  $3d_{5/2}$  and B 1s core levels increase as boron content increases, suggesting a positive chemical shift in the core levels; and (b) the charge-transfer model based on the concept of electronegativity

was not applicable to explain superconductivity in B-excess samples [7].

Although the electronic properties of transition metal diborides have been well studied, details of the electronic structure for  $\text{NbB}_{2+x}$  compounds are not yet completely clear. In this context, it is interesting to probe the theoretical predictions determined from band-structure calculations by performing systematic x-ray photoelectron spectroscopy (XPS) and ultraviolet photoelectron spectroscopy (UPS) experimental studies in order to understand the origin of the superconducting transition in this compound.

## 2. Experimental details

Polycrystalline samples of  $\text{NbB}_{2+x}$  with compositions (B/Nb) = 2.10(1), 2.20(2), 2.30(1), 2.32(1) and 2.34(1) were synthesized by the solid-state reaction method in an Ar atmosphere: preparation details can be found elsewhere [6]. Phase identification of the samples was done using an x-ray Siemens D5000 diffractometer (XRD) using  $\text{Cu K}\alpha$  radiation and an Ni filter. Intensities were measured in steps of 0.02 for 14 s in the  $2\theta$  range  $20^\circ$ – $110^\circ$  at room temperature.

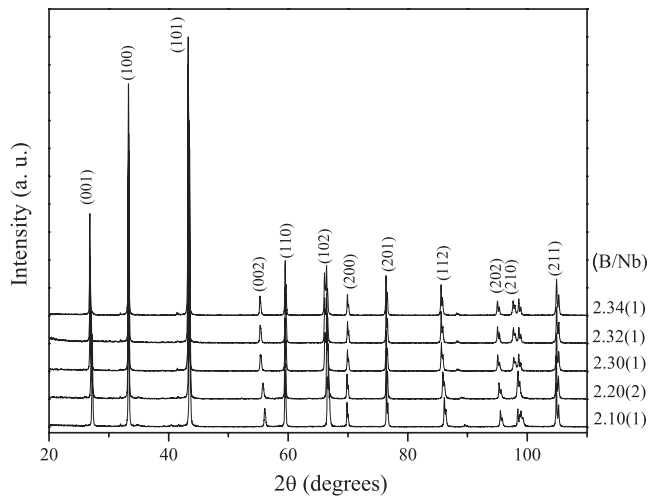


**Figure 1.** X-ray diffraction patterns for the compositions (B/Nb) studied.

Crystallographic parameters were refined using the program Quanto (a Rietveld program for quantitative phase analysis of polycrystalline mixtures) with multi-phase capability [8].

The chemical analysis was carried out by x-ray photoelectron spectroscopy (XPS). This was performed using a VG Microtech ESCA2000 Multilab UHV system, with a  $Mg K\alpha$  x-ray source ( $h\nu = 1253.6$  eV), operated at 15 kV and 20 mA beam with a CLAM4 MCD analyzer. The surfaces of the pellets were etched for 20 min with 4.5 kV  $Ar^+$  at  $0.33 \mu A mm^{-2}$ . XPS spectra were obtained at  $55^\circ$  from the normal surface with a constant analyzer energy (CAE) = 20.0 eV for a high-resolution narrow scan. Peak positions were referenced to the background silver  $3d_{5/2}$  photopeak at 368.0 eV having an FWHM of 1.0 eV, and C 1s hydrocarbon groups in the 284.5 eV central peak position. XPS spectra were fitted with the program SDP v 4.1 [9]. Room temperature ultraviolet photoelectron spectroscopy (UPS) measurements were performed with a CAE = 2.5 eV, using He I ( $h\nu = 21.2$  eV) resonance lines. The XPS error is based considering a detection limit estimated to be 0.1 ppm and uncertainty propagation. For the deconvolution analysis the uncertainty was estimated at 5%.

### 3. Results and discussion

Figure 1 shows the powder x-ray diffraction (XRD) patterns for the compositions (B/Nb) = 2.10(1), 2.20(2), 2.30(1), 2.32(1) and 2.34(1). The main features correspond to the  $NbB_2$  phase (ICDD no. 75-1048). Figure 2 shows the lattice parameters and  $T_c$  for the compositions studied. We observed that the  $a$  parameter decreases slightly as (B/Nb) increases, while the  $c$  parameter increases continuously. As a consequence, the B–B bond length associated with the basal plane decreases slightly, while the Nb–B bond length (along the  $c$  axis) increases continuously. This suggests that the atomic bonding along the  $a$  axis is stronger than that along the  $c$  axis [6]. On the other hand, we observed that  $T_c$  increases as (B/Nb) increases, with a maximum of about 9.8 K for the composition (B/Nb) =

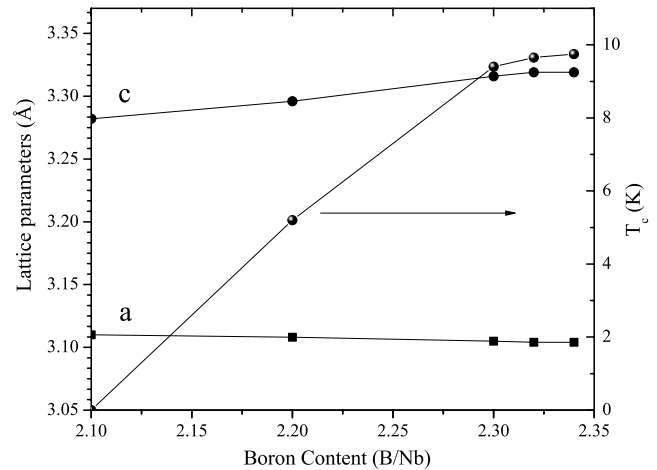


**Figure 2.** Lattice parameters and  $T_c$  as a function of the composition (B/Nb).

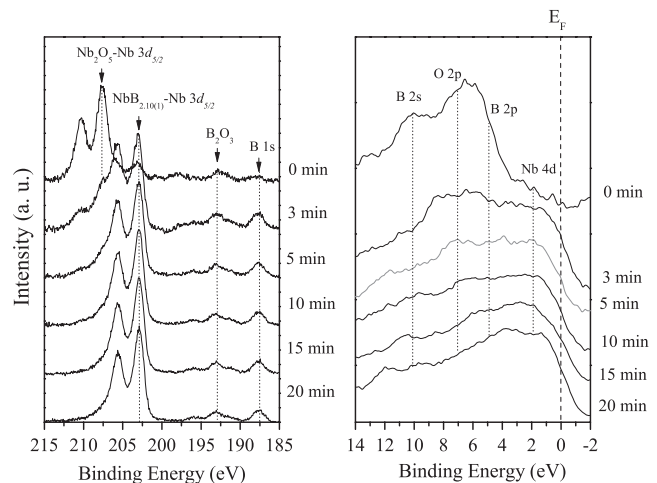


**Figure 3.** XPS spectra Nb 3d core level and valence band as a function of the  $Ar^+$  etching time for the composition (B/Nb) = 2.10(1).

2.34(1) [6]. Accordingly, we supposed that the  $c$  parameter has an important influence on the superconducting behavior of  $NbB_{2+x}$ .

In order to understand the role of chemical state via binding energy core level, we analyzed samples of  $NbB_{2+x}$  by XPS. Figure 3 shows the effect of etching time on the high-resolution XPS spectra of Nb 3d core level and XPS valence band spectra for the composition (B/Nb) = 2.10(1). The surface of the pellets exhibits significant levels of  $Nb_2O_5$  and low levels of  $B_2O_3$ , resulting from the exposure of our samples to air. After etching for 5 min, the  $Nb_2O_5$  layer is removed completely while the  $B_2O_3$  layer remains essentially constant. For etching times longer than 5 min there were no further changes in the Nb 3d core level position, suggesting that the sample stoichiometry remained stable.

Figure 4 shows the high-resolution XPS spectra of Nb 3d core level normalized with respect to the B 1s core level for the samples studied. The Nb  $3d_{5/2}$  core levels were localized at a binding energy (BE) of 203.39, 203.40, 203.54,

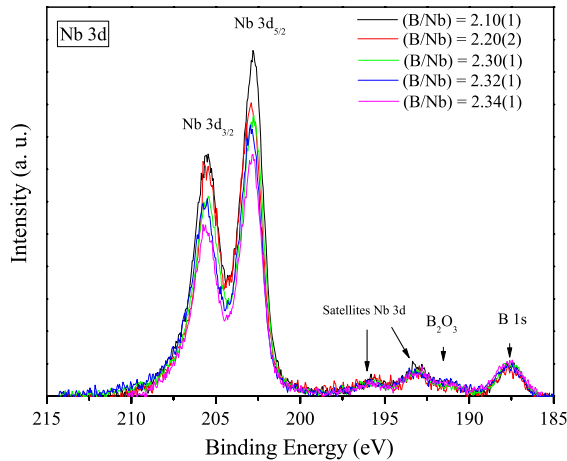


**Figure 4.** XPS spectra Nb 3d core level for the compositions (B/Nb) studied.

203.53 and 203.46 eV for the compositions (B/Nb) = 2.10(1), 2.20(2), 2.30(1), 2.32(1) and 2.34(1), respectively [7]. As we can observe in figure 4, the intensity of the Nb 3d core level decreases as boron content increases. Similar results are observed in XPS studies of non-stoichiometric compounds. For example, in the transition metal carbides and nitrides, the metal or anionic vacancies affect the electronic properties and energy states [10].

In order to determine the effect of boron excess on the density of states (DOS) at the Fermi level  $N(E_F)$  of  $\text{NbB}_2$  we studied the XPS and UPS valence band spectra. Figure 5 shows the XPS and UPS valence band spectra for the compositions from (B/Nb) = 2.10(1) to 2.34(1). To better interpret the spectroscopy data, the valence band spectra are compared with the theoretical DOS of  $\text{NbB}_2$  and  $\text{B}_2\text{O}_3$  determined from band-structure calculations [11, 12]. In the figure, the discontinuous lines limit the niobium and boron states with respect to  $N(E_F)$ . A good correspondence between experiment and theory can be obtained if the DOS is shifted to lower binding energy, as has been done for high-temperature superconductors, where around a 2 eV shift was required. This was attributed to electron correlation effects [13].

If the shifts are done, the feature between 8.0 and 12.0 eV is due to the B 2s bonding states while the feature between 5.0 and 8.0 eV is predominantly due to B 2p bonding states, which are separated from the band of antibonding states associated with Nb 4d states localized at 2.0 eV by a depression [14]. The presence of a depression near  $E_F$  is believed to be due to covalent hybridization between the Nb 4d states and B 2p states [11, 14, 15]. On the other hand, the DOS of  $\text{B}_2\text{O}_3$  shows two bands, the first localized at 9.4 eV and the second at 12.9 eV. The former is associated with hybridization between O 2p states and the B 2p states and the latter to B 2s states [12].

Features of the UPS valence band spectrum for the composition (B/Nb) = 2.34(1) show three main bands centered around 6.4, 9.4 and 12.9 eV. The band centered localized at 6.4 eV was associated with the  $\text{NbB}_2$  phase whereas the others were associated with the  $\text{B}_2\text{O}_3$  phase. As we see in figure 5, the band intensity associated with the  $\text{NbB}_2$

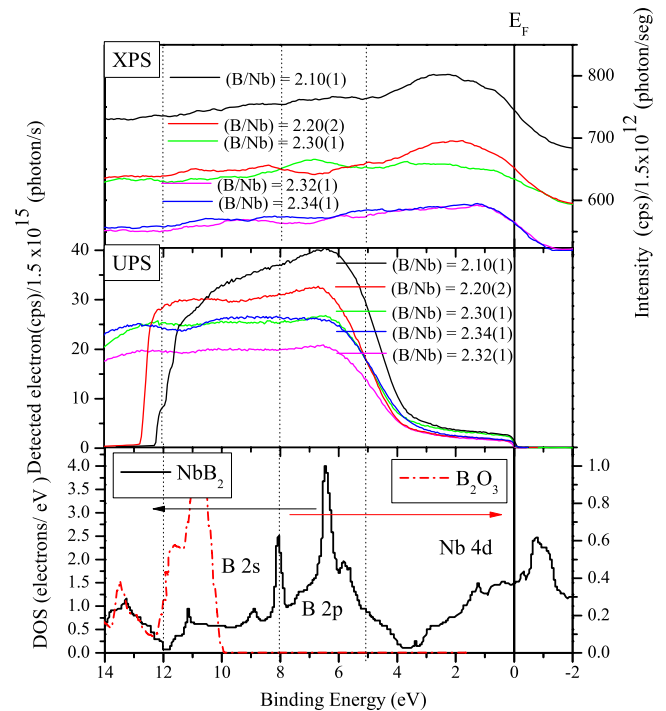


**Figure 5.** Comparison of valence band XPS and UPS spectra function of boron content with the total density of states (DOS) of  $\text{NbB}_2$  [11] and  $\text{B}_2\text{O}_3$  [12].

phase decreases from (B/Nb) = 2.10(1) to 2.34(1) (with a minimum in (B/Nb) = 2.32(1)). However, the intensity of bands associated with the  $\text{B}_2\text{O}_3$  phase increases. Analogous behavior is observed in the XPS valence band spectra where the intensity decreases as the boron content increases.

In spite of the XPS and UPS measurements being performed on polycrystalline samples, the results are representative of the electronic behavior. For example, XPS and UPS studies on superconductors have shown that the valence band and the core level spectra obtained from the single-crystal surfaces are in agreement with spectra recorded from polycrystalline samples [16, 17].

In order to explain the decrease of intensity of the valence band spectra of the compositions studied, we reviewed the results of band-structure calculations on the  $\text{Nb}_{1-x}\text{B}_2$  [11, 18]. The main results of these calculations show that the  $N(E_F)$  for this system decrease with respect to  $\text{NbB}_2$ , whereas near the Fermi level the density of B 2p states increases while that for Nb 4d states decreases. For example, for the composition of  $\text{Nb}_{0.75}\text{B}_2$ , the  $N(E_F)$  decreases 1.9% with respect to  $\text{NbB}_2$ . In this case, the Nb 4d states decreased 16.7% while the B 2p states increased 16.8%. Similar results are observed in the  $\text{TaN}_x$  using density-functional theory [19].

Figure 6 shows the UPS spectra from  $-0.2$  to  $0.2$  eV. As we can see, the tendency of the XPS spectra in the inset is similar to that observed in the UPS spectra. For compositions (B/Nb) = 2.32(1) and 2.34(1) the curves of XPS and UPS spectra at the Fermi level are indistinguishable. From figure 6 we observe that  $T_c$  increases and that  $N(E_F)$  decreases as the compositions (B/Nb) increase. However, it is well known that, in the framework of BCS theory,  $T_c$  is proportional to

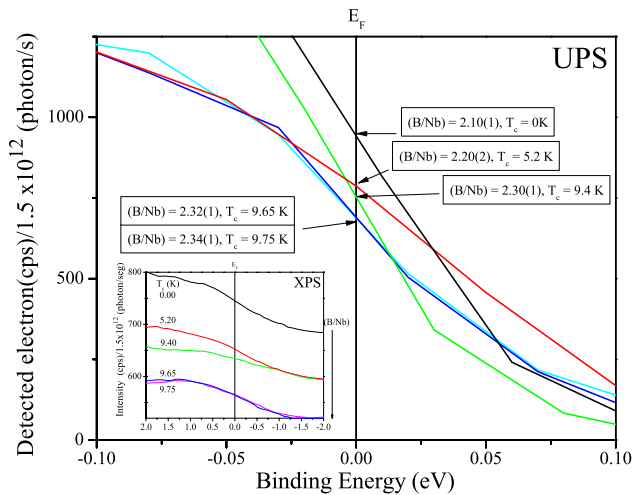


**Figure 6.** UPS spectra at  $N(E_F)$  for the compositions from  $(B/Nb) = 2.10(1)$  to  $2.34(1)$ . Inset shows the XPS spectra for the same compositions.

$\exp(-1/N(E_F)V)$ , where  $V$  is the Cooper pair interaction. For example, in  $MgB_2$  under pressure  $T_c$  decreases as a consequence of  $N(E_F)$  decreasing [20]. Then, we assumed that the increase in  $T_c$  of our compositions studied is not only related to  $N(E_F)$  in spite of the fact that  $NbB_{2+x}$  is a weakly coupled BCS-type superconductor [21].

To explain the appearance of superconductivity in our samples we assumed that the increase of boron content in the  $NbB_{2+x}$  induces vacancies in the Nb layer [22]. It is well known that the presence of superconductivity in the  $MgB_2$  is driven by  $\sigma$  holes in the band passing through the  $\Gamma$ -A direction. These unoccupied states are strongly coupled with lattice vibrations [23]. The DOS near the  $E_F$  is mostly attributed to B  $p_{xy}$  states (band crossing  $E_F$  through the  $\Gamma$ -A line) and B  $p_z$  states (bands crossing  $E_F$  through the  $\Gamma$ -M line) the Mg components near  $E_F$  are actually very small. In  $NbB_2$  the presence of Nb 4d states near  $E_F$  could introduce a covalent character in Nb-B bonds and makes the  $\sigma$  bonding bands sink below the Fermi level [23]. Therefore, the vacancies in niobium can lower the Fermi level and result in additional holes in the  $\sigma$  states. Then, the appearance of superconductivity in  $NbB_{2+x}$  materials might be explained by an increase in carrier density due to an increase in the number of niobium vacancies.

#### 4. Conclusions

Polycrystalline samples of  $NbB_{2+x}$  with compositions  $(B/Nb) = 2.10(1)$ ,  $2.20(2)$ ,  $2.30(1)$ ,  $2.32(1)$  and  $2.34(1)$  were studied by XRD, XPS and UPS. XRD shows that boron excess induces significant changes in the Nb-B bond length, giving rise to an increase in the  $c$  parameter and in  $T_c$ . Analysis of the valence band using XPS and UPS reveals that the boron doping induces a systematic decrease in the  $N(E_F)$  at the Fermi level,

similar to that observed in the  $Nb_{1-x}B_2$  system. This decrease can be associated with a slight decrease in the contribution of the Nb 4d states and to an increase in the contribution of the B 2p states to  $N(E_F)$  as boron content increases. As a consequence, both hole content and  $T_c$  increase.

#### Acknowledgments

We acknowledge support from DGAPA-UNAM under project PAPIIT IN119806-2. Thanks go to Dr M de Llano for carefully reading and correcting the manuscript.

#### References

- [1] Nagamatsu J, Nakagawa N, Muranaka T, Zenitani Y and Akimitsu J 2001 *Nature* **410** 63
- [2] Brewer L, Sawyer D L, Templeton D H and Dauben C H 1952 *J. Am. Ceram. Soc.* **34** 173
- [3] Juretschke H J and Steinitz R 1958 *J. Phys. Chem. Solids* **4** 118
- [4] Cooper A S, Corenzwit E, Longinotti L D, Matthias B T and Zachariasen W H 1970 *Proc. Natl Acad. Sci.* **67** 3132
- [5] Yamamoto A, Takao C, Masui T, Izumi M and Tajima S 2002 *Physica C* **383** 197
- [6] Escamilla R, Lovera O, Akachi T, Duran A, Falconi R, Morales F and Escudero R 2004 *J. Phys.: Condens. Matter* **16** 5979
- [7] Escamilla R and Huerta L 2006 *Supercond. Sci. Technol.* **19** 623
- [8] Altomare A, Burla M C, Giacovazzo C, Guagliardi A, Moliterni A G G, Polidori G and Rizzi R 2001 *J. Appl. Crystallogr.* **34** 392
- [9] 2004 *SDP v4.1 (32 bit)* Copyright XPS International, LLC, Compiled 17 January 2004
- [10] Olaya J J, Huerta L, Rodil S E and Escamilla R 2008 *Thin Solid Films* **516** 8768
- [11] Shein I R, Medvedeva N I and Ivanovski A L 2003 *Phys. Solid State* **45** 1617
- [12] Maslyuk V V, Islam M M and Bredow T 2005 *Phys. Rev. B* **72** 125101
- [13] Likhachev E R, Dubrovskii O I, Kurganskii S I and Domashevskaya E P 1998 *J. Electron Spectrosc. Relat. Phenom.* **88-91** 479
- [14] Vajeeston P, Ravindran P, Ravi C and Asokamani R 2001 *Phys. Rev. B* **63** 045115
- [15] Shein I R and Ivanovski A L 2006 *Phys. Rev. B* **73** 144108
- [16] Shen Z-X, Lindberg P A P, Wells B O, Mitzi D B, Lindau I, Spicer W E and Kapitulnik A 1988 *Phys. Rev. B* **38** 11820
- [17] Vasquez R P, Jung C U, Park M S, Kim H J, Kim J Y and Lee S I 2001 *Phys. Rev. B* **64** 052510
- [18] Xiao R J, Li K Q, Yang H X, Che G C, Zhang H R, Ma C, Zhao Z X and Li J Q 2006 *Phys. Rev. B* **73** 224516
- [19] Stampfl C and Freeman A J 2003 *Phys. Rev. B* **67** 064108
- [20] Islam F N, Islam A K M A and Islam M N 2001 *J. Phys.: Condens. Matter* **13** 11661
- [21] Regalado E and Escamilla R 2007 *J. Phys.: Condens. Matter* **19** 376209
- [22] Nunes C A, Kaczorowski D, Rogl P, Baldissera M R, Suzuki P A, Coelho G C, Grytsiv A, André G, Boureé F and Okada S 2005 *Acta Mater.* **53** 3679
- [23] An J M and Pickett W E 2001 *Phys. Rev. Lett.* **86** 4366